Investigation of the repeatability and reproducibility of hydrophone measurements of medical ultrasound fields

Eleanor Martin, and Bradley Treeby

Citation: The Journal of the Acoustical Society of America **145**, 1270 (2019); doi: 10.1121/1.5093306

View online: https://doi.org/10.1121/1.5093306

View Table of Contents: https://asa.scitation.org/toc/jas/145/3

Published by the Acoustical Society of America

Investigation of the repeatability and reproducibility of hydrophone measurements of medical ultrasound fields

Eleanor Martin[a] and Bradley Treeby
Department of Medical Physics and Biomedical Engineering, University College London, London, WC1E 6BT, United Kingdom

(Received 11 October 2018; revised 14 February 2019; accepted 16 February 2019; published online 7 March 2019)

Accurate measurements of acoustic pressure are required for characterisation of ultrasonic transducers and for experimental validation of models of ultrasound propagation. Errors in measured pressure can arise from a variety of sources, including variations in the properties of the source and measurement equipment, calibration uncertainty, and processing of measured data. In this study, the repeatability of measurements made with four probe and membrane hydrophones was examined. The pressures measured by these hydrophones in three different ultrasound fields, with both linear and nonlinear, pulsed and steady state driving conditions, were compared to assess the reproducibility of measurements. The coefficient of variation of the focal peak positive pressure was less than 2% for all hydrophones across five repeated measurements. When comparing hydrophones, pressures measured in a spherically focused 1.1 MHz field were within 7% for all except 1 case, and within 10% for a broadband 5 MHz pulse from a diagnostic linear array. Larger differences of up to 55% were observed between measurements of a tightly focused 3.3 MHz field, which were reduced for some hydrophones by the application of spatial averaging corrections. Overall, the major source of these differences was spatial averaging and uncertainty in the complex frequency response of the hydrophones.

https://doi.org/10.1121/1.5093306

[KAW] Pages: 1270–1282

I. INTRODUCTION

Accurate measurements of acoustic pressure are essential for characterisation of ultrasonic sources and for experimental validation of models of ultrasound propagation.[1,2] For example, if models of ultrasound propagation are to be used for treatment planning for applications such as transcranial ultrasonic neuromodulation,[3] their accuracy must be validated to ensure that the amplitude and spatial distribution of acoustic pressure can be accurately known at the target location, ensuring that treatments are safe and effective. To begin this process of validation, an ultrasonic source is experimentally characterised, using acoustic holography for example,[4] and supplied as an input to a computational model. The modelled field distribution is then compared to measurements of the ultrasound field after propagation through water or other media.[5] When comparing the measured and modelled pressure, the uncertainties in both the measurements and the model should be considered when deciding if the two are in agreement. Where the model and measurement are not in agreement, then the likely sources of error should be identified and reduced. In this study, factors contributing to errors and uncertainty in the measured pressure are explored.

Currently, the most common method of measuring ultrasound pressure fields is by scanning a hydrophone through the acoustic field of a source transducer using an automated scanning tank. Acoustic pressure is obtained from the measured voltage waveforms by deconvolution of the frequency-dependent sensitivity of the hydrophone over the required bandwidth.[6] Errors in the resulting pressure values can arise from many sources related to the properties of the hydrophone, source, and acoustic field, as well as the processing of the measured data.

Common commercially available hydrophone types include piezoelectric probe and membrane type hydrophones and fibre-optic hydrophones.[7] Membrane hydrophone element sizes range from 0.2 to 0.6 mm and larger, and they typically have a uniform frequency response (in magnitude and phase) over a broad bandwidth.[8,9] Piezoelectric probe type hydrophones are available in a wide range of element sizes from 40 μm to several mm. Both these and fibre-optic hydrophones typically have more variable frequency responses because of diffraction effects around the probe tip.[10–12] Fibre-optic hydrophones have small element sizes (10 or 100 μm) with bandwidth and noise equivalent pressure (NEP) depending on the mode of operation.[13,14]

A suitable hydrophone should be chosen depending on the measurement conditions. For Polyvinylidene fluoride (PVDF) hydrophones, sensitivity increases with element size, but larger element sizes are less omnidirectional and the measurement is the result of pressure averaged over a larger area. This can lead to errors such as underestimation of measured pressure in focused and nonlinear fields and when sound is incident from large angles.[4,15,16] High NEP

[a]Electronic mail: elly.martin@ucl.ac.uk

can limit the use of some hydrophones to measurement of regions of high acoustic pressure.[17] Non-uniformity in hydrophone frequency response causes distortion of nonlinear pressure waveforms, but can be corrected by deconvolution of the complex frequency response of the hydrophone. This has been shown by multiple authors to be important for obtaining accurate acoustic pressure measurements.[13,18–20] However, errors can still arise due to uncertainties in the calibration data, conditioning of the data for the deconvolution process, and stability of the hydrophone sensitivity and frequency response.[21,22]

Other factors associated with the source and measurement set-up can also lead to uncertainty in measurements of acoustic pressure. Fluctuations in electrical impedance and drive voltage, and changes in water temperature, especially during long scans, can result in changes in the acoustic output of transducers contributing to variation in repeated measurements.[4,23] Other factors which could cause variation in measured acoustic pressure include alignment and positioning errors, for example, non-orthogonality of tank axes or imprecise motor positions, reflections from the measurement equipment or the tank or water surfaces, poor water quality, electrical noise, and environmental vibrations.[24]

Previously, the repeatability of field measurements and differences in absolute acoustic pressures measured with different hydrophones have been investigated. One investigation examined fluctuations in transducer drive voltage during measurements, as well as long term stability.[23] This showed variations on the order of 1.5% in both drive voltage and hydrophone voltage over periods of 1 min, and variations of approximately 5% in acoustic pressure measured over the course of a one year period with a membrane hydrophone. A reduction in the variations was achieved by implementing feedback control on the transducer drive voltage. Other authors made repeated measurements of a spherically focused ultrasound field with a piezoceramic hydrophone over a four year period.[17] The coefficients of variation of peak negative and positive hydrophone voltages were 6 and 4% in a 1.05 MHz field, and 4 and 3% in a 3.3 MHz field. The same study also examined differences in acoustic pressure measured by a set of probe hydrophones including a piezoceramic hydrophone plus two fibre-optic and one PVDF hydrophone, with element sizes ranging from 10 to 400 μm. The measured pressures showed differences of up to 42% between hydrophones after deconvolution of their complex frequency responses, and in general, larger variations in the measured pressures were observed at higher drive levels. Another study to assess the agreement between different measurement devices and their suitability for measuring high intensity focused ultrasound (HIFU) fields compared simulations and measurements of two focused ultrasound fields with three different hydrophones at a range of drive levels.[18] Pressures measured with a coated membrane hydrophone (0.2 mm element, 100 MHz bandwidth) and a fibre-optic hydrophone (0.1 mm element, 40 MHz bandwidth) were in good agreement (within 3%) in one field, but differed by approximately 30% in the focal region of a more tightly focused, higher frequency field, underestimating the pressure compared to simulations. It was suggested that the differences were due to spatial averaging and bandwidth limitations.

The aim of the current work is to first quantify the variation in repeated measurements made in our laboratories, and second to examine the variation in acoustic pressure measured with a range of different hydrophones in the fields of several different ultrasound transducers under different driving conditions.

II. METHODS

Two sets of measurements were conducted to assess (1) the repeatability of measurements made under nominally identical conditions, and (2) the reproducibility of acoustic pressure measurements made with a range of hydrophones of different types and sizes under a range of conditions. The aim of the repeatability study was to isolate variations arising from factors outlined in Sec. I, since each hydrophone is compared with itself and the acquisition and processing of waveforms is performed in the same way each time. In the context of metrological studies, reproducibility of measurements is often assessed by comparing measurements made by different users in different laboratories. The aim of the reproducibility study reported here was to capture systematic differences arising due to the properties of each of the hydrophones (including knowledge of the sensitivity), rather than variations between users or laboratories.

A. Hydrophones

Measurements were made with four PVDF hydrophones: a D1602 model 0.2 mm differential membrane hydrophone, a UT1604 model 0.4 mm membrane hydrophone, a 0.2 mm needle hydrophone, and a 40 μm needle hydrophone with hydrophone booster amplifier (all Precision Acoustics Ltd., Dorchester, UK). Magnitude and phase calibrations of the frequency-dependent sensitivity at normal incidence were obtained from the National Physical Laboratory, as detailed in Table I, for all except the 40 μm needle hydrophone. For this hydrophone, a magnitude calibration was provided by Precision Acoustics on purchase. The phase response of the hydrophone was calculated from the measured magnitude sensitivity using the assumption of minimum phase.[25,26] The magnitude and phase of the frequency dependent sensitivity of each hydrophone is shown in Fig. 1.

B. Sources

Three ultrasound transducers were used to provide a variety of different field distributions and frequencies. The first was a single element spherically focusing transducer with aperture diameter 64 mm and focal length 98 mm (H151, Sonic Concepts, Bothell, WA). The transducer was driven at its fundamental frequency of 1.1 MHz, with either a 4 cycle burst or a 40 cycle burst. The second transducer was a single element spherically focusing transducer with aperture diameter 64 mm and focal length 63.2 mm (H101, Sonic Concepts, as before). It was driven at its third harmonic of 3.3 MHz with either a 4 cycle burst or a 120 cycle

TABLE I. Characteristics of the four hydrophones applied to measurement of ultrasound fields in this study. The numbers in brackets denote the frequency interval of the calibrations.

Hydrophone type	Membrane	Needle	Needle	Membrane
Nominal element diameter [μm]	200	40	200	400
Magnitude calibration bandwidth [MHz]	1–40 (1 MHz)	1–30 (1 MHz)	0.1–40 (50 kHz)	0.1 – 1 (50 kHz), 1–40 (1 MHz)
Phase calibration bandwidth [MHz]	1–40 (1 MHz)	–	0.1–40 (50 kHz)	1 – 40 (1 MHz)

burst. For both of these transducers, the input signal was supplied from an Agilent 33522A Arbitrary Waveform Generator (Agilent, Berkshire, UK), amplified by an E&I A075 RF power amplifier (Electronics and Innovation Ltd., Rochester, NY) and coupled to the transducers via their matching networks. Transducer drive voltages were monitored at the input to the transducer matching network with a Tektronix TPP0850 oscilloscope probe and Tektronix DPO5034B digital phosphor oscilloscope (Tektronix, U.K. Ltd., Berkshire, UK). The third transducer was a 128 element diagnostic linear array transducer (L14-5/38, Ultrasonix, Richmond, Canada), with an element pitch of 0.3 mm, and elevation aperture of 4 mm. This was connected to a Sonix MDP ultrasound research scanner (Ultrasonix, as previously) and driven at a frequency of 5 MHz with a 4 cycle burst (waveform configuration +-+-+-+-). Sixteen elements at the centre of the array were driven to create an approximately square aperture, similar to the aperture typically used to generate a single scan line in standard B-mode ultrasound imaging. The focal depth was set to 40 mm.

C. Waveform acquisition and processing

For all measurements, sources were mounted on a two-axis computer controlled rotation stage (θ, ϕ) at a fixed location in an automated scanning tank (Precision Acoustics Ltd., as before) filled with degassed, deionised water. Hydrophones were mounted and positioned with a three-axis (x, y, z) computer controlled translation stage. Waveforms were acquired, digitised, and stored via the digital phosphor oscilloscope, controlled by the scanning tank software, with a sample rate of 100 MHz, and 32 averages. When the transducers were operated in quasi-continuous wave (CW) mode (i.e., driven with a 40 or 120 cycle burst), the hydrophone signal was acquired in a time window occurring after signals from all parts of the transducer had arrived, but before reflections from the measurement equipment had reached the hydrophone. When the transducers were driven with a short pulse (pulsed wave, PW), the hydrophone signal was acquired in a time window that covered both the earliest and latest arrival times of the pulse from all parts of the transducer. To minimise fluctuations in the hydrophone signals due to vibrations generated by movement of the hydrophones by the translation stages during scanning, settle times of up to 5 s were set between acquisitions (this is especially important when scanning the membrane hydrophones along the beam axis). All hydrophones were allowed to soak for at least one hour before measurements were made in line with the manufacturer's recommendations. Water temperature was monitored during all scans and was maintained at 20 ± 1 °C.

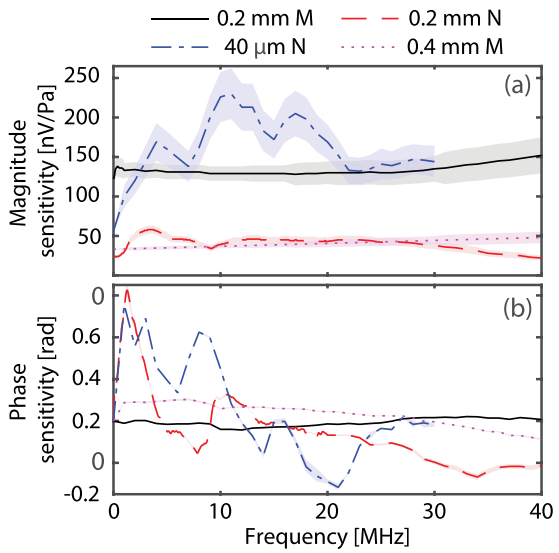

FIG. 1. (Color online) (a) Normal incidence magnitude and (b) phase sensitivity of the four hydrophones used in this study with calibration uncertainties shown as shaded areas. The phase response shown for the 40 μm needle hydrophone (40μm N) was calculated assuming minimum phase. M: membrane, N: needle.

Following acquisition, the waveforms were processed as follows. Steady state signals were cropped to a whole number of cycles and pulsed waveforms were windowed with a Tukey window. The data was bandpass filtered with a −6 dB pass band from 200 kHz to 10 MHz for the 1.1 MHz field, and from 200 kHz to 30 MHz for the 3.3 and 5 MHz fields. The filter was a Tukey window with a 200 kHz taper width which reached the −6 dB cut off 100 kHz into the taper. Filtering and deconvolution of the hydrophone frequency response were implemented by first applying the bandpass filter (Tukey windows) to the double sided Fourier transforms of the waveforms. This was then divided by the complex frequency response of the hydrophones (with phase conjugation) and inverse Fourier transformed to obtain the pressure waveforms.

D. Intra-hydrophone repeatability

For each hydrophone, five sets of repeated measurements were made of the field generated by the H151 transducer with a peak-to-peak drive voltage of 73.4 V, in both pulsed and quasi-continuous wave modes. This generated peak focal pressures of approximately 2.7 MPa and 2.9 MPa in the two modes, respectively, with five harmonics visible in the focal spectra. Each set of measurements consisted of axial and lateral line scans through the focus of the field. Axial line scans were made along the beam axis, from a distance from 40 to 200 mm with a step size of 0.2 mm. Lateral line scans were made from −12 to 12 mm with a step size of

0.2 mm. The measurements were performed over a period of several weeks, and the transducer and hydrophone were removed from the tank then remounted and realigned between each set of measurements, which consisted of scans with each of the test hydrophones. Each hydrophone was aligned to the beam axis by alternately scanning along the two lateral axes through the centre of the −6 dB beam region until the position of the centre was consistent to within approximately 20 μm. For each set of measurements, the transducer beam axis was first aligned with the z-axis of the scanning tank by repeating this process at two axial distances to determine any angular offset, which was then corrected by adjusting the tilt and rotation of the source. For each set of five repeat measurements for each hydrophone, the mean and standard deviation of the peak positive and peak negative pressures were calculated at each scan position. The mean and standard deviation of each sample point in the focal waveforms were also calculated. For this calculation, the waveforms were temporally aligned so the standard deviation reflects only variations in waveform shape and amplitude. The coefficient of variation (the ratio of the standard deviation to the mean, COV) was calculated at the focus, defined as the position of maximum pulse intensity integral.

E. Inter-hydrophone reproducibility

For comparison of the acoustic pressure measurements made by the set of test hydrophones, each of the fields described in Sec. II B was measured with each of the hydrophones. For the two single element transducers, two drive levels were used for both pulsed and steady state measurements. Errors arising from uncertainties in the frequency response and from spatial averaging may be greater in nonlinear fields, so for comparison, the lowest drive level was chosen to generate a linear field, and a higher drive level was chosen to generate four or five harmonics in the focal spectra. For the 1.1 MHz field, the peak-to-peak drive voltages were 7 V and 73.4 V. Axial line scans were made along the beam axis, from a distance from 40 to 200 mm with a step size of 0.2 mm. Lateral line scans were made from −12 to 12 mm with a step size of 0.2 mm. For the 3.3 MHz field, the peak-to-peak drive voltages were 4.3 V and 50.0 V for the steady state measurements and 4.6 V and 50.0 V for the pulsed measurements. Axial line scans were made along the beam axis, from a distance from 40 to 90 mm with a step size of 0.2 mm. Lateral line scans were made from −3 to 3 mm with a step size of 0.05 mm. For the linear array transducer, the power level was set in a MATLAB script in the control software of the scanner. The power level can take values between 0 and 15 and was set at 10. The level was chosen to produce a nonlinear field with spectral amplitude no greater than the noise floor (−42 dB) above 30 MHz (the upper limit of calibration data for the 40 μm needle hydrophone). Lateral line scans were made at a distance of 40 mm from the transducer from −5 to 5 mm with a step size of 0.1 mm.

For all comparisons, the 0.2 mm membrane hydrophone was chosen as the reference hydrophone because of its flat frequency response and smaller element size. For each of the other hydrophones, the difference in the peak positive pressure at each scan point was calculated with respect to the pressure measured by the reference hydrophone, and this difference was divided by the spatial peak pressure measured by this hydrophone

$$L_1(z)[\%] = 100 \times \frac{[p_{\text{ref}}(z) - p_{\text{test}}(z)]}{\max[p_{\text{ref}}(z)]}. \tag{1}$$

Here $p_{\text{ref}}(z)$ is the temporal peak positive or peak negative pressure measured by the reference hydrophone as a function of axial position, z, and $p_{\text{test}}(z)$ is the temporal peak positive or peak negative pressure measured by the test hydrophone as a function of axial position. The root-mean-square (rms) of the difference was also calculated for each scan

$$\epsilon_{\text{rms}}[\%] = 100 \times \frac{\sqrt{\frac{1}{N}\sum [p_{\text{ref}}(z) - p_{\text{test}}(z)]^2}}{\max[p_{\text{ref}}(z)]}, \tag{2}$$

where N is the number of measurements, i.e., the number of positions in each line scan. Both quantities were also calculated for pressure measured as a function of lateral position, x, where z is substituted by x in Eqs. (1) and (2).

F. Hydrophone effective element sizes

It has been previously shown that the effective element sizes of ultrasonic hydrophones are larger than their nominal sizes, particularly at low MHz frequencies.[9,27–29] To assess the impact of this on the measurements, the effective element sizes of the test hydrophones were determined from their measured directional response. For these measurements, the hydrophones were aligned with the beam axis in the far-field of a 39 mm diameter plane piston transducer. The transducer was driven at a frequency of 1 MHz with a 14 cycle burst at an amplitude sufficient to generate multiple harmonics of the driving frequency in the far-field. At the measurement distance (450 mm), the −6 dB beam width was approximately 25 mm, on the order of 60 times the size of the largest nominal hydrophone element. The hydrophones were mounted on a rotation stage with their elements aligned as close as possible to the centre of rotation, and waveforms were acquired at 5° intervals between −70° and +70°. The measurements were then repeated with each hydrophone rotated through 90° about its axis of symmetry. Eight cycles were extracted from each measured waveform starting once the waveform had reached a steady amplitude after the ring-up phase. The fast Fourier transform (FFT) of the waveforms was calculated and the amplitudes of the fundamental and 3rd harmonic were extracted. To obtain the effective element size for each hydrophone at the two frequencies, an optimisation was performed to fit the modelled directional response to the measured directional responses. The directional response of the hydrophones was modelled as

$$D(k,\theta) = \frac{2J_1(ka\sin\theta)}{ka\sin\theta}, \tag{3}$$

which assumes a circular piston in a rigid planar baffle, where J_1 is a first-order Bessel function, k is the wavenumber, a is the element radius, and θ is the angle of incidence

TABLE II. Coefficient of variation [%] of the peak positive (p_+) and peak negative (p_-) pressure measured at the focus for each hydrophone in the field of the H151 transducer driven in both steady state mode (CW) and with a 4 cycle burst (PW). M: membrane, N: needle.

		Hydrophone			
		0.2 mm M	40 μm N	0.2 mm N	0.4 mm M
CW	p_+	0.9	0.9	1.8	0.4
	p_-	1.0	1.3	1.4	0.4
PW	p_+	1.0	0.7	1.9	0.5
	p_-	1.1	0.8	1.8	0.5

of the beam on the element. The fitting was repeated for each set of measurements and the effective element size was obtained from the mean of the two sets of measurements for each hydrophone at each frequency.

To investigate the impact of spatial averaging over the effective element sizes of the hydrophones on field measurements, the fields of the H101 and H151 transducers were modelled using the FOCUS MATLAB toolbox using the fast near field method.[30,31] The transducers were modelled as spherical shells, with aperture diameter 61.4 mm and radius of curvature 63.2 mm for the H101 transducer, and aperture diameter 62.2 mm and radius of curvature 99.1 mm for the H151 transducer. These parameters were previously derived for the transducers by fitting the modelled responses to measurement data.[5] The resulting modelled pressure was then averaged over a disk of varying size corresponding to the hydrophone effective element sizes. Note, since this particular model does not include nonlinear propagation, the results were compared only with the lowest drive level CW field.

III. RESULTS

A. Intra-hydrophone repeatability

Overall, the variations between repeated measurements were small for all of the hydrophones. The coefficient of variation of the temporal peak positive and peak negative pressure at the focus was less than 2% for all hydrophones under both pulsed and steady state conditions as shown in Table II. The peak-to-peak drive voltage measured before and after each measurement varied by less than 0.4%. The coefficient of variation of the peak pressures was very similar for the two drive modes for all of the hydrophones. The 0.4 mm membrane hydrophone showed the least variation, with COVs of 0.4 and 0.5% for steady-state and pulsed conditions, respectively. This hydrophone may be less sensitive to misalignment with the beam axis due to its larger element size. The largest variations were seen with the 0.2 mm needle hydrophone with COVs of 1.8 and 1.9%.

Figure 2 shows the mean axial and lateral profiles and mean focal waveform for each hydrophone for the CW

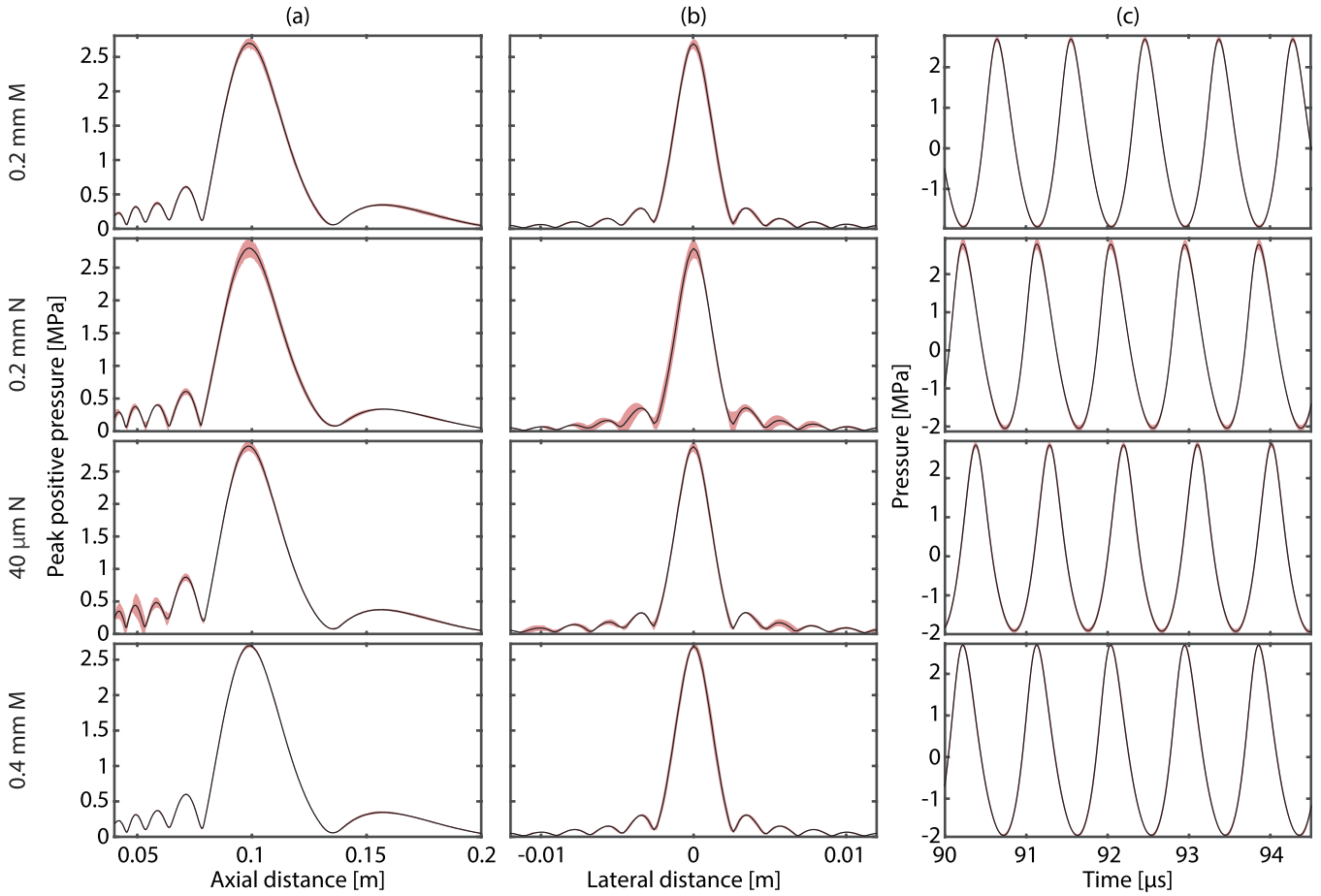

FIG. 2. (Color online) Measurements of the field of the H151 single element bowl transducer at 1.1 MHz in steady state mode made with the four test hydrophones. (a) Mean axial peak positive pressure. (b) Mean lateral peak positive pressure. (c) Mean focal waveform. Solid lines show averaged measurements ($n = 5$), shaded area denotes the mean ± 3 standard deviations of the mean. M: membrane, N: needle.

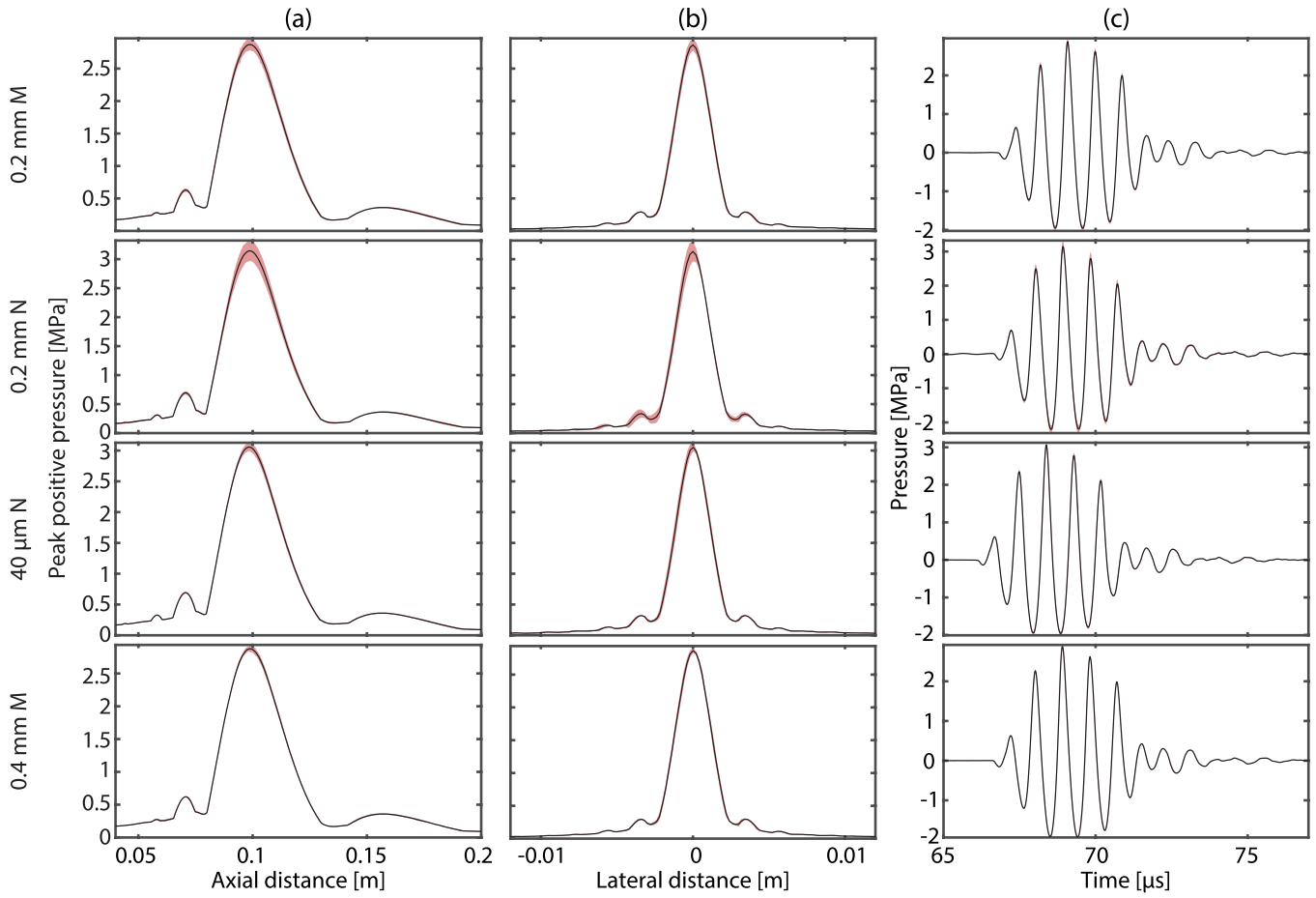

FIG. 3. (Color online) Measurements of the field of the H151 single element bowl transducer at 1.1 MHz in pulsed mode made with the four test hydrophones. (a) Mean axial peak positive pressure. (b) Mean lateral peak positive pressure. (c) Mean focal waveform. Solid lines show averaged measurements ($n = 5$), shaded area denotes the mean ± 3 standard deviations of the mean. M: membrane, N: needle.

measurements. The shaded areas on each plot show ± 3 standard deviations, which gives the 99.7% confidence interval. The same is shown for the PW measurements in Fig. 3. For the CW measurements, outside of the focal region, variations can be seen in the prefocal and side lobes of the field. These are more pronounced for the needle hydrophones, while the measurements made with the membrane hydrophones are more consistent. The amplitude of the pre-focal maxima and minima could be affected by errors in the alignment to the beam axis and by reflections from the hydrophone and mounts so may vary from measurement to measurement when the hydrophone is remounted. The field distribution is simpler when the transducer is driven with a short pulse, as sound arriving from different parts of the transducer surface will be at least partially temporally separated and so does not interfere to create the axial peaks and nulls seen in the CW field. The COV is less than 2% up until the pressure decreases at the far end of the profiles where the COV increases. There is greater variation in the lateral scans, which is most obvious for the 0.2 mm needle hydrophone, with the COV rising to more than 10% as the distance from the beam axis increases. In this direction, the field varies on a smaller spatial scale than in the axial direction, so small differences in the hydrophone position in the field between scans have a greater effect. The NEP obtained for each hydrophone with the averaging used in measurements was approximately 6 kPa, approximately 0.2% of the peak focal pressure. At the low, linear drive level, this is approximately 3% of the peak pressure so may contribute to larger variations in measurements made at lower drive levels.

B. Inter-hydrophone reproducibility

For the inter-hydrophone comparison, differences between the peak focal pressure measured by each hydrophone and the reference hydrophone (0.2 mm membrane) are summarised for each transducer, drive level, and mode in Table III.

1. H151 driven at 1.1 MHz

For the low-level linear measurements in both CW and PW modes, the focal peak positive pressures agreed closely. The largest difference in focal pressure compared to the reference hydrophone was for the 0.4 mm membrane hydrophone in PW mode at 3.6%. In the CW mode, the focal peak pressure measured with the needle hydrophones agreed with the reference hydrophone to within the three standard deviation level described in Sec. III A. For the 0.4 mm membrane, the difference is larger than this, but the differences are still small at 1.6 and 3.0% for the peak positive pressures and 3.0

TABLE III. Temporal peak positive and negative pressures measured at the focus by the 0.2 mm membrane hydrophone and relative differences in the pressures measured by each of the hydrophones. L_1 focus gives the relative differences in peak positive (p_+) and peak negative (p_-) pressures at the focus [%], ϵ_{rms} are the rms differences in temporal peak positive pressure as a percentage of the focal peak pressure measured by the 0.2 mm membrane hydrophone. M: membrane, N: needle.

		CW				PW			
	Difference metric	Pressure [MPa] 0.2 mm M	Difference [%] 40 μm N	0.2 mm N	0.4 mm M	Pressure [MPa] 0.2 mm M	Difference [%] 40 μm N	0.2 mm N	0.4 mm M
H151	L_1 focus p_+	0.22	2.9	0.2	−1.6	0.23	1.5	3.5	−3.0
1 MHz	L_1 focus p_-	0.21	2	−0.7	−3	0.22	1.7	2.7	−3.6
	ϵ_{rms} axial		3.7	1.5	0.9		1.0	1.5	1.2
	ϵ_{rms} lateral		1.6	1.9	1.6		1.2	0.9	1.6
	L_1 focus p_+	2.7	6.4	1.7	−0.3	2.9	6.3	10.7	0.5
	L_1 focus p_-	1.9	−0.4	5.6	−2.4	2.0	−0.4	13.9	−1.6
	ϵ_{rms} axial		3.4	0.9	0.3		1.9	3.6	0.2
	ϵ_{rms} lateral		1.5	0.8	0.9		1.2	1.9	0.3
H101	L_1 focus p_+	0.27	48.1	26.6	−18.7	0.22	37.0	29.3	−15.0
3.3 MHz	L_1 focus p_-	0.26	46.5	26.2	−18.4	0.21	38.7	28.8	−14.3
	ϵ_{rms} axial		12.3	6.7	4.4		9.0	7.2	3.5
	ϵ_{rms} lateral		24.5	5.3	4.6		10	13.9	4.9
	L_1 focus p_+	3.6	37.3	54.6	−21.8	2.7	31.3	46.6	−16.0
	L_1 focus p_-	2.7	20.1	46.5	−17.9	2.1	23.0	41.6	−13.9
	ϵ_{rms} axial		9.4	11.9	4.3		7.4	10.1	3.5
	ϵ_{rms} lateral		19.9	9.3	4.5		7.9	14.4	4.7
L14-5	L_1 focus p_+					0.77	2.5	5.9	−2.1
5 MHz	L_1 focus p_-					0.48	−12.4	6.9	−3.3
	ϵ_{rms} lateral						1.8	4.0	2.8

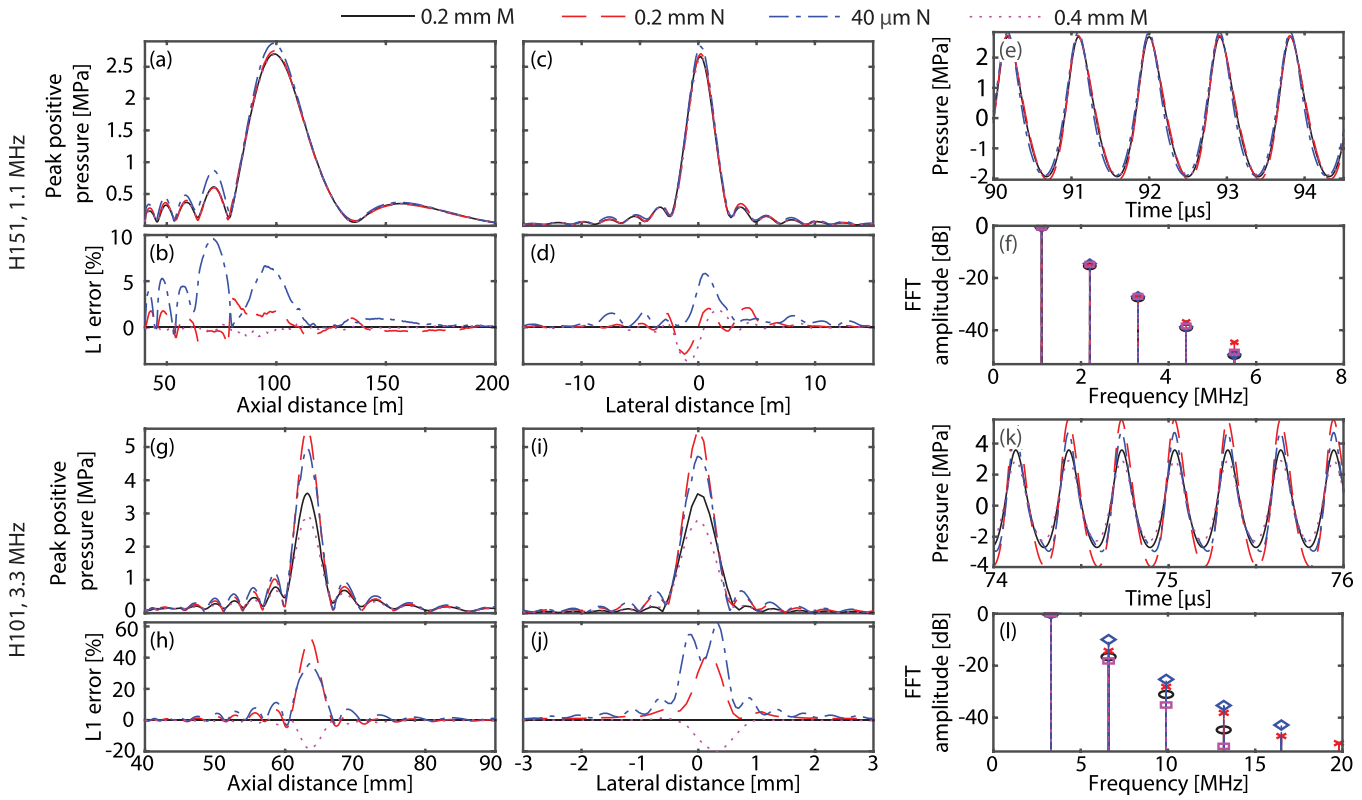

FIG. 4. (Color online) Measurements of the field of single element bowl transducers in steady state mode made with the four test hydrophones. For H151 at 1.1 MHz: (a) Axial peak positive pressure and (b) L_1 error at each scan point. (c) Lateral peak positive pressure and (d) L_1 error at each scan point. (e) Focal waveforms and (f) spectra. For H101 at 3.3 MHz: (g) Axial peak positive pressure and (h) L_1 error at each scan point. (i) Lateral peak positive pressure and (j) L_1 error at each scan point. (k) Focal waveforms and (l) spectra. M: membrane, N: needle.

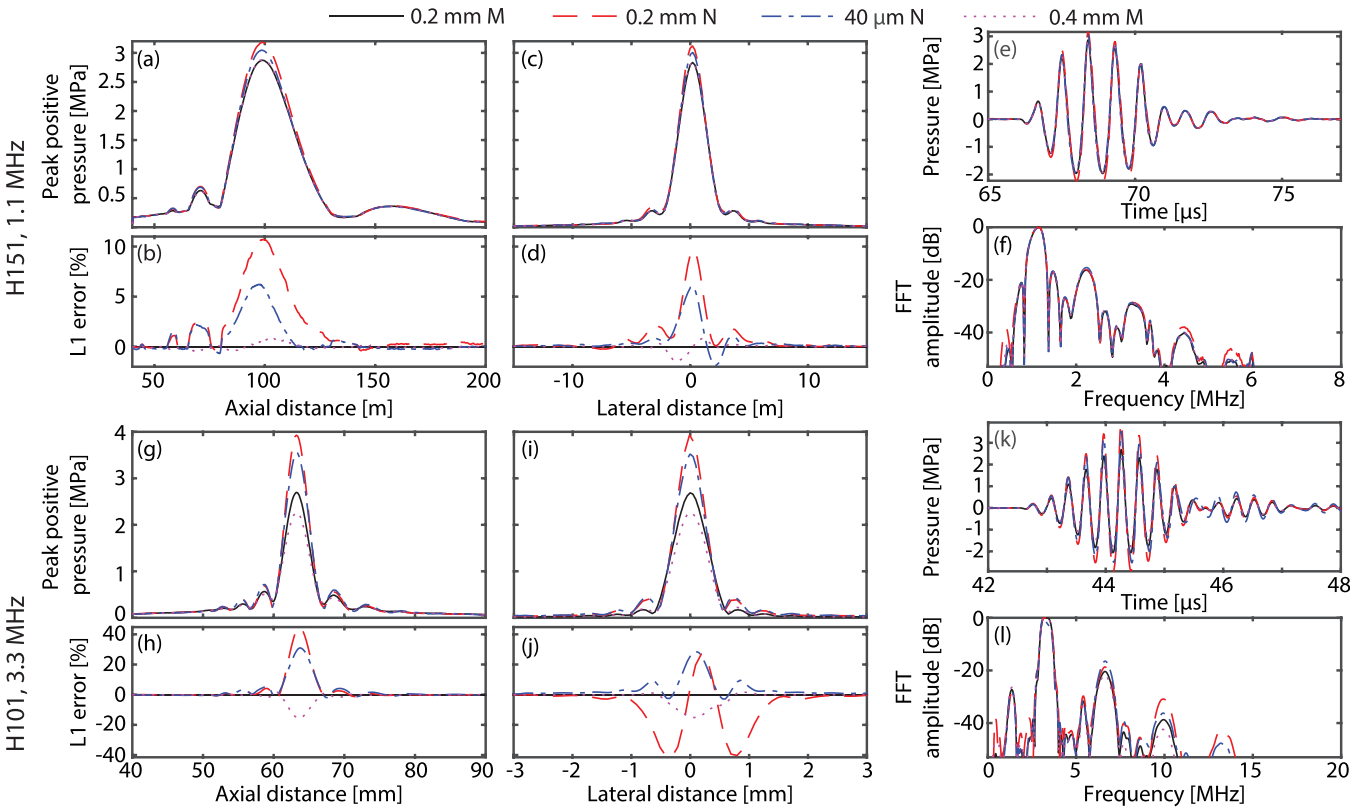

FIG. 5. (Color online) Measurements of the field of single element bowl transducers in pulsed mode made with the four test hydrophones. For H151 at 1.1 MHz: (a) Axial peak positive pressure and (b) L_1 error at each scan point. (c) Lateral peak positive pressure and (d) L_1 error at each scan point. (e) Focal waveforms and (f) spectra. For H101 at 3.3 MHz: (g) Axial peak positive pressure and (h) L_1 error at each scan point. (i) Lateral peak positive pressure and (j) L_1 error at each scan point. (k) Focal waveforms and (l) spectra. M: membrane, N: needle.

and 3.6% for the peak negative pressures in CW and PW modes, respectively. The rms differences over the lateral and axial profiles are less than 2% for all except the CW axial profile measured by the 40 μm needle hydrophone. In this case, there are differences of 10%–15% in the amplitude of the prefocal maxima, which increases the rms difference to 3.7%. These differences may be due to the more omnidirectional response of the needle hydrophone. Closer to the transducer, waves are incident from a greater range of angles, so the lower sensitivity of the larger hydrophones at large angles of incidence may result in lower pressure amplitudes in these regions. At the higher drive level, there were larger differences in the focal pressure as shown in Figs. 4 and 5. Again, the largest differences are seen in the prefocal lobes for the 40 μm hydrophone. There are larger differences in focal pressure between the needle hydrophones and the reference hydrophone, up to 10.7 and 13.9% (p_+, p_-) for the 0.2 mm needle hydrophone for the PW mode. It is not clear why the difference in focal pressure is so much greater for this hydrophone in PW mode compared to CW mode. The pressure amplitude is slightly higher and there is energy visible at higher frequencies in the spectrum of the short pulse so the increased amplitude measured at those frequencies could have a greater effect on the focal pressure amplitude.

2. H101 driven at 3.3 MHz

For the 3.3 MHz field, there are large differences in the profiles measured by the different hydrophones. The peak focal pressures vary by up to 55% and there are differences in the amplitude and position of maxima and minima in both the lateral and axial profiles (see Figs. 4 and 5). At the lower drive level, both needle hydrophones measured higher focal pressures than the reference hydrophone. The highest pressure was measured by the 40 μm needle hydrophone (CW: +48.1%, PW +37%), and the lowest by the 0.4 mm membrane (CW: −18.7%, PW −15.0%). At the higher drive level, the highest pressure was measured by the 0.2 mm needle hydrophone (CW: +54.6%, PW +46.6%). The differences between the 0.4 mm membrane hydrophone and the reference hydrophone are similar for both drive levels. In addition to differences in the pressure at the focus, in the CW axial profiles, the amplitudes of the pre and post focal maxima measured by the membrane hydrophones are about 25% lower than for the needle hydrophones, and the minima are higher. In the lateral profiles, the distance from the beam axis to the minimum at the edge of main beam is greater for the membrane hydrophones and the amplitude of the sidelobes are approximately 35%–50% lower. For the 40 μm needle hydrophone, larger differences were observed in the CW measurements than in the PW measurements and these were larger at the lower, linear drive level in contrast to the differences seen for the other hydrophones and drive conditions. Magnitude only calibration data was obtained for this hydrophone, measured in 1 MHz steps, and the phase response was subsequently calculated from the magnitude response using the assumption of minimum phase. As can be

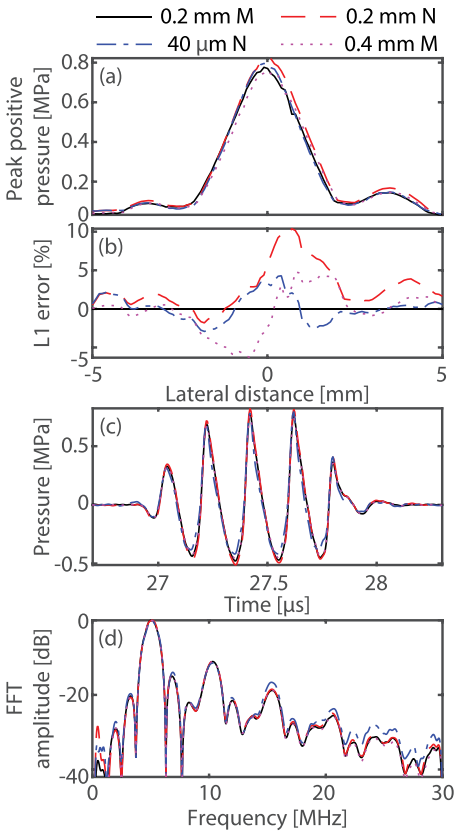

FIG. 6. (Color online) Measurements of the field of the L14-5 linear array transducer driven with a short pulse at 5 MHz made with the four test hydrophones. (a) Lateral peak positive pressure, (b) L_1 error profile, (c) focal waveforms, and (d) spectra. M: membrane, N: needle.

seen from Fig. 1, both the magnitude and phase response vary significantly over the frequency range. The unknown frequency response between the measured steps together with the estimated phase response leads to greater uncertainty, likely to have greater impact on deconvolution of the frequency response from nonlinear and broadband pulses.

3. L14–5 driven at 5 MHz

The beam profiles and focal waveforms and spectra measured by each of the four test hydrophones in the 5 MHz linear array field are shown in Fig. 6. The differences in focal pressure measured by the different hydrophones (relative to the reference hydrophone) are moderate: −2.1 and −3.3% for the temporal peak positive and peak negative pressures for the 0.4 mm membrane, 2.5 and −12.4% for the

TABLE IV. Effective element sizes determined from measurement of directional response of the test hydrophones at 1 and 3 MHz. M: membrane, N: needle.

Hydrophone	Effective element diameter [μm]	
	1 MHz	3 MHz
40 μm N	470	175
0.2 mm N	620	330
0.2 mm M	1700	675
0.4 mm M	1550	750

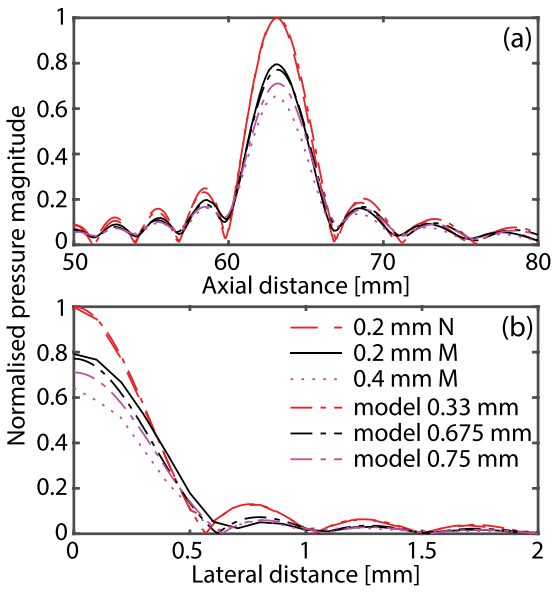

FIG. 7. (Color online) Measured and modelled (a) axial and (b) lateral profiles through the focus of the field generated by the H101 transducer driven in CW mode at 3.3 MHz. Profiles were modelled using the transducer parameters and measured effective element sizes. Measured profiles are normalised to the 0.2 mm needle measurements, modelled profiles are normalised to the 0.33 mm element data. M: membrane, N: needle.

40 μm needle hydrophone, and 5.9 and 6.9% for the 0.2 mm needle hydrophone. The shape of the focal waveform measured by the 40 μm hydrophone is slightly different to the others with the temporal peak pressure on the fourth cycle rather than the third as for the other waveforms. The peak negative pressure is also lower for this hydrophone, and differences can be seen in the spectrum of the waveform where the relative amplitude of the harmonics increases with frequency compared to the other hydrophones.

C. Hydrophone effective element sizes

The effective element sizes of the hydrophones obtained from fitting to measurements of their directional responses at 1 and 3 MHz are shown in Table IV. For all hydrophones, the effective element sizes are larger than their nominal sizes, by up to ten times at 1 MHz and four times at 3 MHz. These element sizes are consistent with those previously measured for similar hydrophones. For needle hydrophones, the increase in effective element size at low frequencies is likely due to diffraction around the needle and other edge effects.[27] For membrane hydrophones, the increase is likely to be due to the propagation of Lamb waves in the membrane.[8,32] Beard *et al.*[27] measured the effective element size of a similar 0.2 mm needle hydrophone as approximately 600 μm in diameter at 1 MHz and 300 μm in diameter at 3 MHz. Yoshioka *et al.*[28] measured the effective element size of a similar nominal 0.4 mm diameter membrane hydrophone at 5 MHz as 0.9 mm (average diameter), and Radulescu *et al.*[29] and Wilkens and Molkenstruck[9] also measured effective element sizes larger than their nominal sizes for a range of membrane and probe-type hydrophones. There are also other models that include effects other than spatial

averaging in the directional response, which result in effective element sizes closer to nominal values.[33]

The effects of spatial averaging on the 3.3 MHz field when using different hydrophones is shown in Fig. 7. The 3.3 MHz field used in this study is tightly focused with a −6 dB beam width of approximately 0.6 mm. This is on the order of the element sizes of the hydrophones, leading to significant spatial averaging effects for all hydrophones except for the 40 μm hydrophone, for which the decrease in focal pressure is predicted to be approximately 3% compared to a point sensor. The 40 μm hydrophone was omitted from the comparison due to the apparent inconsistency in its behaviour. The measured axial and lateral beam profiles were normalised to the maximum of the 0.2 mm needle hydrophone profile (the smallest element size), and the modelled profiles were normalised to the maximum of the modelled profile given by the effective element size of the 0.2 mm needle hydrophone.

The relative decreases in focal pressure and smoothing of the axial and lateral profiles seen for the membrane hydrophones relative to the 0.2 mm needle hydrophone are similar to those predicted by the modelled profiles. The beam width increases and sidelobe amplitude decreases in both the measured and modelled profiles as the element size increases. These results are consistent with the significant spatial averaging effects previously observed in measurements of a nominally identical transducer driven at 3.32 MHz when compared to the modelled field.[34] In an investigation of the effects of spatial averaging including nonlinear propagation, modelled data was averaged over the effective hydrophone element area at increasing drive levels. It was shown that when there is significant nonlinearity in the field, averaging over the high frequency value of the effective element size (usually close to the nominal element size) agrees well with measured data, at least for the peak positive pressure, where there is a strong dependence on the high frequency components of the wave.

The beam width of the H151 1.1 MHz field is approximately 3 mm and the effects of spatial averaging are less visible. For the 1.1 MHz field, the model shows that spatial averaging leads to decreases in pressure of less than 2% for the needle hydrophones and leads to a drop of about 10% in the amplitude of the focal pressure compared to a point sensor for the membrane hydrophones. This could explain the differences observed between these measured profiles although they are not as large as predicted by the model.

In IEC 62127[2] and IEC 62556,[24] it is recommended that the effective element radius of the hydrophone should be less than a quarter of a wavelength at the acoustic working frequency, which is approximately 350 μm at 1.1 MHz and 113 μm at 3.3 MHz. It also gives the following relationship for calculating the maximum effective hydrophone radius when this is not practical:

$$a_{\mathrm{hyd}} = \frac{\lambda}{8\,a_{\mathrm{tx}}}\left(z^2 + a_{\mathrm{tx}}^2\right)^{1/2}, \tag{4}$$

where λ is the wavelength at the acoustic working frequency, a_{tx} is the transducer aperture radius, and z is the distance between the source aperture and hydrophone. This means that at the geometric focal distance, the maximum effective element radius should be less than 560 μm for the H151 transducer at 1 MHz, and 130 μm for the H101 transducer at 3.3 MHz. For the 1.1 MHz field, the effective element sizes of both membrane hydrophones exceed this limit, and for the 3.3 MHz field, all hydrophones except the 40 μm needle hydrophone exceed the limit if the effective element size at the acoustic working frequency is considered. Note, IEC 62556 does not explicitly state that the maximum effective hydrophone radius should relate to the acoustic working frequency, only that it is dependent on frequency. However, given the results presented here which show spatial averaging effects for those hydrophones exceeding these maximum effective radii, it appears that for fields with little or no nonlinearity, the effective hydrophone radius at the acoustic working frequency is the most relevant quantity.

D. Spatial averaging corrections

IEC 62127 defines a method for applying corrections to the measured spatial peak pressure to compensate for spatial averaging.[2] Assuming the radial field distribution close to the axis can be modelled as a quadratic function, a correction is applied based on the ratio of the measured peak positive pressure at one or half the hydrophone radius from the beam axis to the on-axis pressure. The correction factor is given by

$$K_{sa} = (3 - \beta)/2, \tag{5}$$

where β is the ratio of the signal at one hydrophone radius from the axis to the signal on axis. K_{sa} is valid for $\beta > 0.8$, which in this case applies only to the two needle hydrophones based on their effective radii. For the membrane hydrophones and all hydrophones where there is nonlinearity in the field, the correction factor is given by

$$K'_{sa} = (3 - 2\beta'), \tag{6}$$

where β' is the ratio of the signal at half the hydrophone radius from the axis to the signal on axis.

To examine the impact of spatial averaging corrections, the corrections given in Eqs. (5) and (6) were calculated and applied to the measured and modelled 3.3 MHz field data. The temporal peak positive pressure measured by the 0.2 mm hydrophone and the relative differences in the pressure measured by the membrane hydrophones, before and after correction for spatial averaging, are shown in Table V for both the CW and PW measurements. The spatial peak pressure modelled for the 0.2 mm hydrophone, normalised by the spatial peak pressure predicted for a point sensor, and the relative differences in the pressures modelled for the other hydrophones before and after correction for spatial averaging are also shown.

For the measured data, in both the CW and PW cases, the spatial averaging correction increases the temporal peak pressure measured by the 0.2 mm needle hydrophone by approximately 9.5%. For the membrane hydrophones, the application of the correction reduces the relative differences

TABLE V. Temporal peak positive pressures measured at the focus by the 0.2 mm needle hydrophone and modelled for the 0.2 mm and relative differences in the pressures measured and modelled by the 0.2 and 0.4 mm membrane hydrophones, before and after correction for spatial averaging. The pressure modelled for the 0.2 mm needle hydrophone is normalised to the spatial peak pressure amplitude predicted for a point sensor. M: membrane, N: needle.

		Pressure [kPa]	Difference [%]	
		0.2 mm N	0.2 mm M	0.4 mm M
CW	Measured	342	20.9	35.2
	Corrected	374	7.0	19.9
PW	Measured	288	22.5	34.0
	Corrected	316	8.3	18.2
		Normalised pressure	Difference [%]	
CW	Modelled	0.92	22.9	28.9
	Corrected	0.99	8.4	12.4

from 21 to 7% and from 35 to 20% for the 0.2 and 0.4 mm hydrophones, respectively. The changes are similar for the PW case. For the modelled data, the correction has a very similar effect for the 0.2 mm membrane hydrophone measurements, reducing the difference relative to the 0.2 mm needle hydrophone from 23 to 8%. For the 0.4 mm membrane hydrophone, the relative difference was smaller before correction compared to the measurements, and the application of the correction reduces this further from 29 to 12%.

The modelled data predicts that before any correction for spatial averaging, the 0.2 mm needle hydrophone underestimates the pressure by 8% compared to a point sensor. After application of the spatial averaging correction, the difference in the predicted peak pressure amplitude reduces to less than 1% relative to a point sensor. This suggests that the application of spatial averaging corrections is effective for this hydrophone.

The application of spatial averaging corrections introduces further uncertainty in the pressure measured by the hydrophones. For $\beta' > 0.92$, the uncertainty on the correction is estimated to be 10%. This is the case for the corrections calculated for the needle hydrophone. For comparison, the uncertainty in the magnitude sensitivity at 3.3 MHz is 9% for this hydrophone. For the membrane hydrophones, the calculated correction factors are between 28 and 35% and have larger associated uncertainties. The disparities still remaining after application of spatial averaging corrections to the membrane hydrophones, both in measurement and modelling, and the large uncertainties associated with the corrections, suggest that for these hydrophones the corrections are not fully effective. The standard states that where the −6 dB beam width is less than 1.5 times the effective hydrophone diameter, it is important that a smaller hydrophone is used. This is the case for both membrane hydrophones in this situation, and this recommendation is supported by the data shown here.

IV. DISCUSSION

For all hydrophones, the coefficient of variation of the spatial and temporal peak positive and peak negative pressures was less than 2%. This is comparable with the variation in repeated measurements performed in other similar studies.[17,23] Three standard deviations of the mean gives the 99.7% confidence interval, so almost all measurements can be expected to lie within this range. Except for the measurements of the field of the H151 transducer at 1.1 MHz at the lowest drive level, the differences between the pressures measured with the needle and membrane hydrophones were greater than three times the coefficient of variation. This suggests that the differences were not due only to random uncertainties arising from changes in hydrophone sensitivity or source output, or from alignment of the source and hydrophone. The differences were slightly larger when the field contained some nonlinearity, which may be due to uncertainties in the frequency response of the hydrophones both in terms of the absolute value and the variation with frequency.

The uncertainties on the calibrations of the hydrophones used in this study ranged from 6 to 15% for magnitude sensitivity and was on the order of 5 to 30 mrad for phase sensitivity across the calibration bandwidths. It should be noted that the uncertainty in the phase sensitivity provided with the calibration was estimated from the random uncertainties only, and that the true uncertainty will therefore be larger. For the 40 μm needle hydrophone, the uncertainty on the magnitude sensitivity is larger in practice due to its nonuniform frequency response in combination with calibration data obtained only in steps of 1 MHz, likely leading to errors in the values assumed between these steps. In addition, the phase sensitivity was calculated from the minimum phase theorem for this hydrophone. While it has been demonstrated that this approach agrees well with the directly measured phase, there can be larger differences at the upper and lower frequency ends of the calibration data.[26] Additionally, it is not trivial to determine how uncertainty in magnitude and phase sensitivity propagates through the deconvolution process to uncertainty in the resulting pressure waveforms.[22,35] Considering the uncertainty in magnitude sensitivity only, which is more valid for the linear field conditions, for the 1.1 MHz and 5 MHz fields, it appears that the differences in the peak pressures measured by the different hydrophones are in most cases well within the calibration uncertainties. The two membrane hydrophones measured very similar pressures at both drive levels in these fields, possibly due to their similar construction and their similarly flat frequency responses.

The differences in the measurement of the 3.3 MHz field for the H101 transducer were larger, up to 55%. However, the pressure measurements in the broadband field of the L14–5 linear array transducer were all within 9%, suggesting that the differences observed in the 3.3 MHz fields were not solely due to uncertainties in the frequency responses of the hydrophones. The differences observed here were comparable to the variations observed by Wear *et al.*[19] when measuring broadband ultrasound pulses with a range of membrane and probe type hydrophones. In that study, the same model of transducer was used and at a similar drive level. There were differences of up to 30% in the focal peak positive pressure measured by the test hydrophones, which for at least one of the hydrophones was thought to be partially due

to spatial averaging effects. The field of this transducer is tightly focused, with a −6 dB beam width of 0.6 mm, and in the current study, the largest hydrophone element size was 0.4 mm. The observed differences in measured pressure are consistent with the simulated effects of spatial averaging for these hydrophones.

The application of spatial averaging corrections as defined in IEC 62127 reduces the differences in the temporal peak pressure measured by the different hydrophones. For the 0.2 mm needle hydrophone, after the application of spatial averaging corrections, the spatial peak pressure was within 1% of that predicted for a point sensor, showing that for this hydrophone, the correction is effective. However, for the membrane hydrophones, which had the largest element sizes, differences from 7 to 8% remained after correction of the measured and modelled data for the 0.2 mm membrane hydrophone and differences from 12 to 20% remained for the 0.4 mm membrane hydrophone relative to the 0.2 mm needle hydrophone. This suggests that the spatial averaging corrections are not completely effective in this case. It is recommended in the standard that when the hydrophone element diameter is greater than two thirds of the −6 dB beam width, which is true for the membrane hydrophones in this field, a smaller hydrophone should be used.

For the L14-5 field at 5 MHz, the effective element sizes of the hydrophones are smaller than at 1 and 3 MHz, and the −6 dB beam width is approximately 2.5 mm, so spatial averaging effects should be small. The field is broadband, with energy up to 30 MHz in the spectrum. As shown by Wilkens *et al.*,[34] due to the contribution of high frequency harmonics to the peak pressure in nonlinear fields, spatial averaging effects are likely to be consistent with the high frequency value of the hydrophone effective element size, which usually approaches the nominal hydrophone element size. This effect and the broadness of the beam in this case are consistent with the smaller differences observed between the measurements of this field with the different hydrophones. The waveforms and profiles measured by the different hydrophones agree well, with some differences seen in the focal waveform shape and spectrum of the 40 μm hydrophone. This may be explained by the increased uncertainty in the frequency response of this hydrophone, which was non-uniform but measured only in steps of 1 MHz with phase calculated using the minimum phase theorem rather than directly measured. The differences observed here are comparable to the differences in acoustic pressure measured in a broadband 3 MHz field (−6 dB beamwidth ∼3 mm) by eight probe and membrane hydrophones, with element sizes ranging from 10 μm to 1 mm reported by Wear *et al.*[19] After deconvolution of their complex frequency responses, the coefficient of variation of the measured peak positive and negative pressures were 8 and 9%. The variations were attributed to spatial averaging effects, hydrophone positioning, and calibration uncertainties, which were quoted as 10% for one of the hydrophones.

V. CONCLUSION

It has been shown that repeatable measurements can be made with a variety of hydrophones in a 1.1 MHz spherically focused ultrasound field with a beam width of 3 mm. The stability of the hydrophones and sources, together with careful alignment, enable repeatable measurements, with peak pressures expected to lie within 3% of the mean. Obtaining reproducible and correct absolute acoustic pressure measurements was shown to be more challenging. Differences between the pressures measured with different hydrophones were greater when the fields contained some nonlinearity compared to those observed in linear fields. The greatest differences were shown to be due to spatial averaging in a tightly focused field (frequency 3.3 MHz, −6 dB beam width ∼0.6 mm). The effective element sizes of all hydrophones were shown to be larger than their nominal values. Application of spatial averaging corrections to the needle hydrophone measurements reduced the resulting underestimation of the pressure and the discrepancy between these measurements.

The membrane hydrophones used in this study are often considered as reference hydrophones due to their stability and uniform frequency responses. However, it has been shown that at low frequencies, their effective element sizes are far larger than their nominal element sizes. This should be taken into consideration when evaluating their suitability for measurement of pressure varying on a small spatial scale. IEC 62127 states that when the ratio of the beam width to effective element size is less than 1.5, as is the case for these hydrophones in tightly focused fields, a smaller hydrophone should be used, as the uncertainties in the spatial averaging corrections will be large. The results suggest that accurate quantitative characterisation of nonlinear focused ultrasound fields requires hydrophones with small element sizes in addition to the application of spatial averaging corrections for most commercially available PVDF hydrophones. Fibre-optic hydrophones with small element sizes could be more suitable in these cases, providing their frequency response is stable and well characterised. Alternatively, it may be necessary to apply deconvolution of the full complex angular frequency response of the hydrophones.[36] In general, the results of this study suggest that, in the cases tested at least, spatial averaging is the largest source of measurement error, and when spatial averaging is not significant or appropriate spatial averaging corrections are applied, broadband fields can be measured with differences of less than 10% with a range of hydrophones, as long as their complex frequency response is known over the required bandwidth and in steps that capture variations on the correct scale.

ACKNOWLEDGMENTS

This work was supported by the Engineering and Physical Sciences Research Council (EPSRC), UK, Grant Nos. EP/P008860/1 and EP/L020262/1.

[1]W. Kreider, P. Yuldashev, O. A. Sapozhnikov, N. Farr, A. Partanen, M. Bailey, and V. A. Khokhlova, "Characterization of a multi-element clinical HIFU system using acoustic holography and nonlinear modeling," IEEE Trans. Ultrason. Ferroelectr. Freq. Control **60**(8), 1683–1698 (2013).

[2]IEC 62127-1: *Ultrasonics—Hydrophones: Part 1: Measurement and Characterization of Medical Ultrasonic Fields up to 40 MHz* (IEC, Geneva, Switzerland, 2013).

[3]W. Legon, L. Ai, P. Bansal, and J. K. Mueller, "Neuromodulation with single-element transcranial focused ultrasound in human thalamus," Human Brain Mapp. **39**(5), 1995–2006 (2018).
[4]O. A. Sapozhnikov, S. A. Tsysar, V. A. Khokhlova, and W. Kreider, "Acoustic holography as a metrological tool for characterizing medical ultrasound sources and fields," J. Acoust. Soc. Am. **138**(3), 1515–1532 (2015).
[5]E. Martin, Y. Ling, and B. Treeby, "Simulating focused ultrasound transducers using discrete sources on regular cartesian grids," IEEE Trans. Ultrason. Ferroelectr. Freq. Control **63**(10), 1535–1542 (2016).
[6]A. Hurrell, "Voltage to pressure conversion: Are you getting 'phased' by the problem?," J. Phys. Conf. Ser. **1**, 57–62 (2004).
[7]A. Hurrell and P. Beard, "Piezoelectric and fibre-optic hydrophones," in *Ultrasonic Transducers*, edited by K. Nakamura (Woodhead Publishing, Oxford, UK, 2012), Chap. 19, pp. 619–676.
[8]S. Robinson, R. Preston, M. Smith, and C. Millar, "PVDF reference hydrophone development in the UK-from fabrication and lamination to use as secondary standards," IEEE Trans. Ultrason. Ferroelectr. Freq. Control **47**(6), 1336–1344 (2000).
[9]V. Wilkens and W. Molkenstruck, "Broadband PVDF membrane hydrophone for comparisons of hydrophone calibration methods up to 140 MHz," IEEE Trans. Ultrason. Ferroelectr. Freq. Control **54**(9), 1784–1791 (2007).
[10]A. Hurrell, "Finite difference modelling of acoustic propagation and its application in underwater acoustics," Ph.D. thesis, University of Bath, Bath, UK, 2002.
[11]P. Morris, A. Hurrell, and P. Beard, "Moving towards an ideal frequency response with fibre-optic hydrophones," in *Proceedings of the IEEE International Ultrasonics Symposium 2009*, Roma, Italy (September 20–23, 2009), pp. 944–947.
[12]W. Weise, V. Wilkens, and C. Koch, "Frequency response of fiber-optic multilayer hydrophones: Experimental investigation and finite element simulation," IEEE Trans. Ultrason. Ferroelectr. Freq. Control **49**(7), 937–946 (2002).
[13]M. S. Canney, M. R. Bailey, L. A. Crum, V. A. Khokhlova, and O. A. Sapozhnikov, "Acoustic characterization of high intensity focused ultrasound fields: A combined measurement and modeling approach," J. Acoust. Soc. Am. **124**, 2406–2420 (2008).
[14]P. Morris, A. Hurrell, A. Shaw, E. Zhang, and P. Beard, "A Fabry-Perot fiber-optic ultrasonic hydrophone for the simultaneous measurement of temperature and acoustic pressure," J. Acoust. Soc. Am. **125**(6), 3611–3622 (2009).
[15]B. Zeqiri and A. D. Bond, "The influence of wave-form distortion on hydrophone spatial-averaging corrections—Theory and measurement," J. Acoust. Soc. Am. **92**(4), 1809–1821 (1992).
[16]M. A. Ghanem, A. D. Maxwell, W. Kreider, B. W. Cunitz, V. A. Khokhlova, O. A. Sapozhnikov, and M. R. Bailey, "Field characterization and compensation of vibrational non-uniformity for a 256-element focused ultrasound phased array," IEEE Trans. Ultrason. Ferroelectr. Freq. Control **65**(9), 1618–1630 (2018).
[17]Y. Liu, K. A. Wear, and G. R. Harris, "Variation of high-intensity therapeutic ultrasound (HITU) pressure field characterization: Effects of hydrophone choice, nonlinearity, spatial Averaging and Complex Deconvolution," Ultrasound Med. Biol. **43**(10), 2329–2342 (2017).
[18]J. Haller, K.-V. Jenderka, G. Durando, and A. Shaw, "A comparative evaluation of three hydrophones and a numerical model in high intensity focused ultrasound fields," J. Acoust. Soc. Am. **131**(2), 1121 (2012).
[19]K. A. Wear, P. M. Gammell, S. Maruvada, Y. Liu, and G. R. Harris, "Improved measurement of acoustic output using complex deconvolution of hydrophone sensitivity," IEEE Trans. Ultrason. Ferroelectr. Freq. Control **61**(1), 62–75 (2014).
[20]V. Wilkens and C. Koch, "Amplitude and phase calibration of hydrophones up to 70 MHz using broadband pulse excitation and an optical reference hydrophone," J. Acoust. Soc. Am. **115**(6), 2892 (2004).
[21]A. Hurrell and S. Rajagopal, "The practicalities of obtaining and using hydrophone calibration data to derive pressure waveforms," IEEE Trans. Ultrason. Ferroelectr. Freq. Control **64**(1), 126–140 (2017).
[22]S. Eichstädt and V. Wilkens, "Evaluation of uncertainty for regularized deconvolution: A case study in hydrophone measurements," J. Acoust. Soc. Am. **141**(6), 4155–4167 (2017).
[23]J. Haller and V. Wilkens, "Short- and longtime stability of therapeutic ultrasound reference sources for dosimetry and exposimetry purposes," AIP Conf. Proc. **1821**, 180001 (2017).
[24]IEC TS 62556:2014: *Ultrasonics—Field Characterization—Specification and Measurement of Field Parameters for High Intensity Therapeutic Ultrasound (HITU) Transducers and Systems* (IEC, Geneva, Switzerland, 2014).
[25]K. A. Wear, P. M. Gammell, S. Maruvada, Y. Liu, and G. R. Harris, "Time-delay spectrometry measurement of magnitude and phase of hydrophone response," IEEE Trans. Ultrason. Ferroelectr. Freq. Control **58**(11), 2325–2333 (2011).
[26]K. A. Wear, P. M. Gammell, S. Maruvada, Y. Liu, and G. R. Harris, "Comparison of hydrophone phase response obtained via time delay spectrometry measurement and Hilbert transformation," AIP Conf. Proc. **1481**, 450–456 (2012).
[27]P. C. Beard, A. M. Hurrell, and T. N. Mills, "Characterization of a polymer film optical fiber hydrophone for use in the range 1 to 20 MHz: A comparison with PVDF needle and membrane hydrophones," IEEE Trans. Ultrason. Ferroelectr. Freq. Control **47**(1), 256–264 (2000).
[28]M. Yoshioka, "Difference between nominal and measured active element sizes of hydrophones," Jpn. J. Appl. Phys. **47**(5), 3926–3928 (2008).
[29]E. G. Radulescu, P. A. Lewin, A. Nowicki, and W. A. Berger, "Hydrophones' effective diameter measurements as a quasi-continuous function of frequency," Ultrasonics **41**(8), 635–641 (2003).
[30]J. F. Kelly and R. J. McGough, "Transient field generated by spherical shells in viscous media," in *Proceedings of the 8th International Symposium on Therapeutic Ultrasound*, Minneapolis, MN (September 10–13, 2008), pp. 210–214.
[31]D. Chen and R. J. McGough, "A 2D fast near-field method for calculating near-field pressures generated by apodized rectangular pistons," J. Acoust. Soc. Am. **124**(5), 1526–1537 (2008).
[32]D. R. Bacon, "Characteristics of a PVDF membrane hydrophone for use in the range 1–100 MHz," IEEE Trans. Sonics Ultrason. **29**(1), 18–25 (1982).
[33]K. A. Wear, C. Baker, and P. Miloro, "Directivity and frequency-dependent effective sensitive element size of needle hydrophones: Predictions from four theoretical forms compared with measurements," IEEE Trans. Ultrason. Ferroelectr. Freq. Control **65**, 1781–1788 (2018).
[34]V. Wilkens, S. Sonntag, and O. Georg, "Robust spot-poled membrane hydrophones for measurement of large amplitude pressure waveforms generated by high intensity therapeutic ultrasonic transducers," J. Acoust. Soc. Am. **139**(3), 1319–1332 (2016).
[35]S. Eichstädt and V. Wilkens, "GUM2DFT—A software tool for uncertainty evaluation of transient signals in the frequency domain," Meas. Sci. Technol. **27**, 055001 (2016).
[36]E. Martin, E. Z. Zhang, J. A. Guggenheim, P. C. Beard, and B. E. Treeby, "Rapid spatial mapping of focused ultrasound fields using a planar Fabry-Pérot sensor," IEEE Trans. Ultrason. Ferroelectr. Freq. Control **64**(11), 1711–1722 (2017).